International Journal of Chemical Studies

P-ISSN2349–8528
E-ISSN 2321–4902
IJCS 2016; 4(5): 98-105
© 2016 JEZS
Received: 15-07-2016
Accepted: 16-08-2016

Dr. Sana Ahmad
Department of Chemistry, Lahore College for Women University, Lahore, Pakistan

Aamna Ashraf
Department of Chemistry, Lahore College for Women University, Lahore, Pakistan

Correspondence
Dr. Sana Ahmad
Department of Chemistry, Lahore College for Women University, Lahore, Pakistan

Solar assisted photocatalytic degradation of crystal violet and methylene blue dyes using ZnO/SBA-16 as catalyst

Dr. Sana Ahmad and Aamna Ashraf

Abstract
In the present work, mesoporous SBA-16 was synthesized using tetraethyl orthosilicate as the silica source, triblock co-polymer Pluronic F127 as template and cetyltrimethylammonium bromide (CTAB) as co-template respectively. The surface modification of SBA-16 was carried out by impregnation of zinc oxide. As-prepared SBA-16 and ZnO/SBA-16 were characterized by FTIR, TGA, BET and SEM techniques. Characterization techniques revealed that zinc oxide was highly dispersed into/over the well-ordered mesoporous channels and even after impregnation of zinc oxide, mesostructure of SBA-16 was still retained together with high thermal stability, high surface area, large pore volume and uniform pore size. The catalytic activity of the ZnO/SBA-16 was investigated for degradation of methylene blue dye and analyzed by UV-Vis spectroscopy. The results showed that as-prepared ZnO/SBA-16 exhibited excellent catalytic activity towards degradation of crystal violet and methylene blue dye.

Keywords: SBA-16, mesoporous material, photocatalyst, methylene blue, photo degradation

1. Introduction
Dyes are widely used at commercial level, particularly in the industries such as cosmetic industries, textile, paper and pulp and leather industries etc. According to an estimation, approximately 7×10^5 tons of dyes are produced annually for commercial use which consist of greater than 100,000 dyes. These are usually non-degradable and have toxic effects on fauna and flora. Many dyes causes skin irritation, allergic dermatitis, dysfunction of brain, liver, kidney, central nervous system and reproductive system. Some dyes are mutagenic and carcinogenic [1]. E- Methylene blue and crystal violet are hazardous dyes and both are stable under ambient conditions. Both dyes have widespread applications in industries such as leather, textile/dyeing, paper, ballpoint pen, foodstuffs, analytical chemistry and cosmetics. Investigations reveal that CV is carcinogenic in nature as it causes cancer in human bladder.
The presence of MB dye in waste water is hazardous for our environment. Its exposure can cause vomiting, eye infection, diarrhea and nausea. Long term exposure of this dye through consumption, inhalation and by skin contact can disrupt reproductive and central nervous system. Hence wastewater containing harmful dyes should be treated before coming in contact with environment [2]. These are also harmful for aquatic life.
There are different technologies for the removal of dyes from water. These include conversion of the dye pollutant from a liquid state to another state, filtration process, reverse osmosis, electrolysis, adsorption of dye on a suitable adsorbent so that it can be or incinerated or disposed of in a junkyard. However these technologies has some drawbacks e.g., filtration membranes have limited life time after which membrane fouling occurs.
Photocatalytic degradation is another remedy for the dye removal. This technique leads to the complete dissociation of the dye pollutant and has been investigated extensively [3]. This technology is used in this research work for degradation of crystal violet dye. Recent studies have shown that semiconductors can be used as heterogeneous photocatalyst for the removal of dyes from water. This application is based on the principle that when a semiconductor is illuminated with an appropriate light source, the electrons are promoted to the conduction band, which leaves positive holes in the valence band. The generated electron–hole pairs can recombine or move to the surface of the semiconductor to induce reactions in which organic dye can be degraded.

Although TiO_2 has been the most popular semiconductor photocatalyst, ZnO has also been widely investigated in recent years. ZnO has numerous advantages compared to TiO_2. It absorbs a larger fraction of the UV spectrum and more light quanta and it has lower cost and higher photocatalytic efficiencies for the degradation of some organic pollutants in water. Its application in photocatalysis is limited by a wide band gap (3.37eV), instability in acid conditions, low mechanical and thermal stability, and aggregation of nanoparticles which leads to low surface area and reduction in photo catalytic efficiency [4]. It absorbs only 4–5% of solar spectrum lying in the Ultra Violet range, so the use of zinc oxide in the presence of solar energy particularly visible light still remains a challenge. In ZnO photo generated holes and electrons recombine very fast which cause hindrance to the photo catalytic efficiency [5]. In order to avoid these limitations researchers have made many efforts. These include preparation of nanoparticles, combination with other semiconductors [4] and use of host material such as porous glasses, colloidal solutions, alumina and polymers. Several studies have been reported on the preparation of ZnO composites by attaching or impregnating ZnO into a stable inorganic material with a developed surface, such as carbon nanomaterials, clay, zeolites, mesoporous silicas.

Mesoporous silicas are most suitable support materials for loading semiconductor nanoparticles, as they have high hydrothermal and chemical stability, ordered framework, adjustable pore size and large surface area which prevents aggregation of nanoparticles [6]. Among mesoporous silicas, SBA-16 has 3-dimensional cage like structure in a cubic arrangement (Im3m space group) where "each mesopore is connected to eight neighboring mesoporous by microporous channels" [8]. It has thick walls (up to 9nm) and large pores (5-15nm). Due to these thick walls SBA-16 has high stability.

In this paper we have reported the synthesis of SBA-16 using tetraethyl orthosilicate as the silica source, triblock co-polymer Pluronic F127 as template and cetyltrimethylammonium bromide (CTAB) as co-template respectively. Zinc oxide was introduced into SBA-16 mesoporous silica framework by incipient wetness impregnation method (IWI). The photo degradation activity of ZnO/SBA-16 was evaluated for the degradation of crystal violet dye under sunlight.

2. Experimental

2.1 Materials and Methods

Pluronic F127 surfactant was purchased from Sigma-Aldrich Tetraethyl orthosilicate (TEOS) was obtained from Fluka, cetyltrimethylammonium bromide (CTAB) was purchased from BDH, Hydrochloric acid (Merck), Zinc Nitrate ($Zn(NO_3)_26H_2O$, 98%) from Riedel-de Haën® and methylene blue dye from Sigma-Aldrich. All solvents were of analytical grade and used without further purification. Deionized water was used in the present study.

2.2 Synthesis of SBA-16

Mesoporous silica SBA-16 was synthesized under reflux using tetraethyl orthosilicate (TEOS) as source of silica, cetyltrimethylammonium bromide as co-surfactant, triblock co-polymer Pluronic F127 as template. F127 (1.26g, 0.52mmol) and CTAB (0.14g, 0.38mmol) were dissolved into 100mL of 2 M HCl solution, then TEOS (4g, 19.20mmol) was added and the solution was magnetically stirred under refluxing condition for 6 h at 40°C and then at 80°C for another 6 h. The resulting products were obtained by centrifugation at 2000 rpm for 10 min and washed with ethanol 3 times. The product was then dried in a furnace at 80°C for 6h. The sample was then calcined for 6h at 550°C for removal of surfactants [8].

2.3 Synthesis of ZnO/SBA-16

Zinc oxide was incorporated into SBA-16 mesoporous silica framework by using incipient wetness impregnation method**.** SBA-16 (0.3 g) was treated with a zinc nitrate aqueous solution (0.675g in $5cm^3$) under magnetic stirring at room temperature for 45 min and then treated in ultrasonic bath for 20 min. The resulting solid was then filtered in sintered glass crucible, washed with ethanol twice and then dried at 40 ˚C in oven for 5 h and then calcined at 500 ˚C for 2 h with heating rate of 2 ˚C/min.

2.4 Characterization methods:

As-synthesized SBA-16 and ZnO/SBA-16 were characterized by using techniques named as Fourier Transform Infrared (FT-IR) spectroscopy, Thermo Gravimetric Analysis (TGA), Scanning Electron Microscopy (SEM) and Nitrogen adsorption/desorption technique.

2.5 Photo degradation experiments

In all the degradation tests, 50 ml of methylene blue dye solution having initial concentrations in the range 15ppm to 50 ppm was taken in photocatalytic vessel. 30mg of as-prepared photocatalyst was added in each batch and the pH of the solutions was adjusted to 4, 6, 8, 10 and 11. Then the resulting samples were stirred in dark for 30min in order to obtain adsorption-desorption equilibrium.

The whole setup was then kept in sunlight for 2h in the month of August and September. After every 30 min, 5 ml of sample was drawn and the suspended particles of catalyst were removed by centrifugation. Degradation of methylene blue dye was also studied using parent SBA-16 and in the absence of catalyst. The concentration of crystal violet was determined by UV–Vis spectrophotometer at 663nm.

3. Results and Discussion

3.1 FT-IR analysis

Fourier transform-infra red spectra of all the samples were collected by using M2000 MIDAC USA FT-IR instrument. The spectrum of SBA-16 is depicted in Fig 1. The expected bands at $462m^{-1}$ and $809cm^{-1}$ indicates the symmetric bending and stretching vibrations for Si-O-Si bonds [9]. The vibrational band at 964 cm^{-1} indicates the presence of silanol groups (Si–OH) in mesoporous silica [10]. The peaks at $1095cm^{-1}$ and $1388cm^{-1}$ were assigned to the asymmetric stretching vibration of Si-O-Si bond [9]. The band appearing at 1643 cm^{-1} is attributed to the O-H bending vibration indicating the presence of water molecules either present in KBr or in the sample.

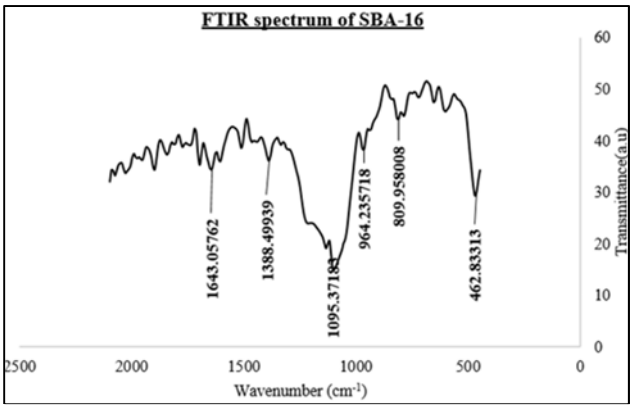

Fig 1: FT-IR spectrum of SBA-16

Fig 2 shows the FTIR spectrum of zinc oxide incorporated SBA-16. It can be seen that asymmetric stretching vibration of Si-O-Si shifted to lower wave number 1087cm^{-1} from 1095cm^{-1}. This may be due to incorporation of zinc oxide into the SBA-16 mesoporous silica.

The band at 964 cm^{-1} was significantly reduced for ZnO/SBA-16 as compared to SBA-16. This may be due to the formation of bonds between Si–OH groups and zinc oxide on the surface of SBA-16 [10].

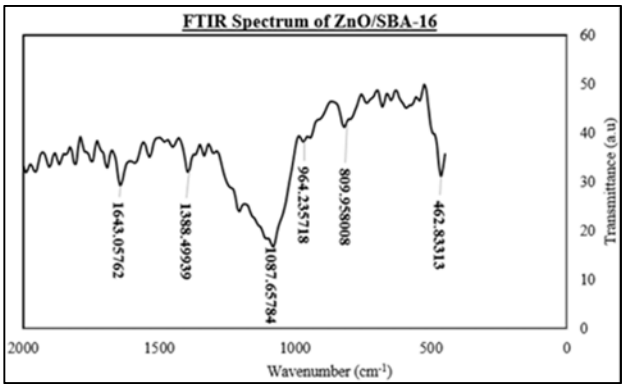

Fig 2: FT-IR spectrum of ZnO/SBA-16

3.2 SEM analysis

Scanning electron microscopic images of all the samples were recorded using JEOL JSM-6480LV instrument working at 20KV.The SEM images of the as-prepared SBA-16 mesoporous silica are shown in Fig. 3 (a) and (b). It can be seen that spherical particles are obtained having large surface area and uniform morphology. Although a little particle aggregation is observed, yet no big clusters are present in the sample. Due to the highly porous structure, SBA-16 becomes an attractive candidate as catalytic support as it facilitates the incorporation of functional groups, heteroatoms, metals and metal oxides.

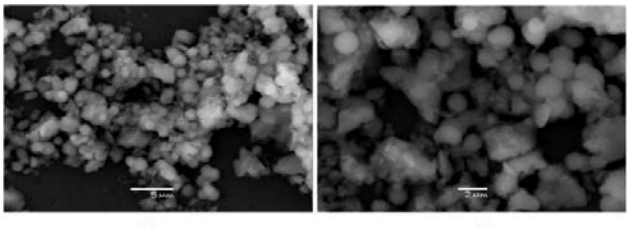

Fig 3: (a) and (b) show SEM images of mesoporous silica SBA-16

Fig.4 (a) and (b) shows SEM images of ZnO/SBA-16. It can be seen that small zinc oxide nanoparticles are homogenously dispersed on the surface of SBA-16. Some irregularities in the structure of ZnO/SBA-16 are observed indicating little particle aggregation.

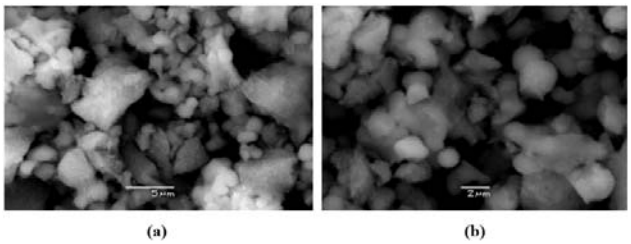

Fig 4: Figure (a) and (b) show SEM images of ZnO/SBA-16

The change in the morphology of ZnO/SBA-16 could be due to agglomeration of zinc oxide particles inside the pores of SBA-16 mesoporous silica.

3.3 Thermogravimetric analysis

Thermogravimetric plots of all the samples were collected using TGA instrument SDT Q600 with temperature rise of 10 degree per minute from 25 to 1000 ºC under nitrogen atmosphere. Figure 5 shows TGA plot of parent SBA-16. Initial 9.8% weight loss from 25ºC to 125ºC is due to decomposition of adsorbed water. From 125ºC to 600ºC only 2.3% weight loss was observed which corresponds to the thermal decomposition of F127 (template) and CTAB (co-template) [10]. After 600 ºC no significant mass loss was observed. Hence it can be concluded that as-prepared SBA-16 exhibited excellent thermal stability.

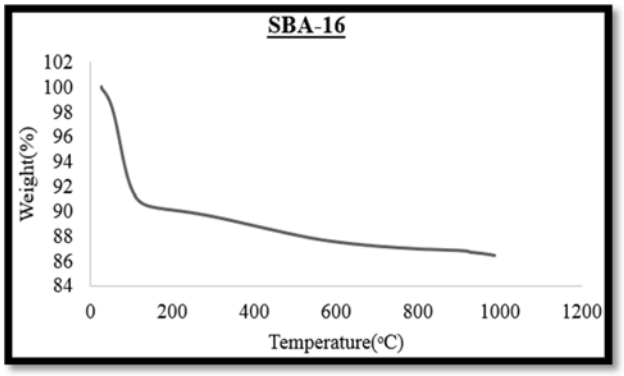

Fig 5: Thermogravimetric analysis of SBA-16

Figure 6 shows the TGA curve for zinc oxide supported SBA-16. The major weight loss (about 9.7%) between 25 ºC and 125ºC was due to evaporation of physically adsorbed water. Another 2% mass loss between 125ºC and 600 ºC was observed which was attributed to the decomposition of F127 template and CTAB co-template which remained unclaimed during calcination step [10].

After 600 ºC, no mass loss was observed indicating high thermal stability of the material. Hence it can be concluded that even after the incorporation of zinc oxide, SBA-16 silica retains its thermal stability and resulting as-prepared catalyst ZnO/SBA-16 also has high thermal stability.

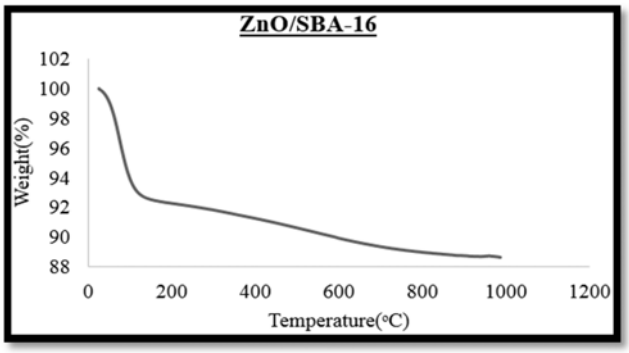

Fig 6: TGA curve of ZnO/SBA-16

3.4 N_2 adsorption/desorption analysis:

Pore size distribution and BET surface area were measured using BET instrument TriStar II 3020. Nitrogen was used as adsorptive gas at 77.300K.

BET surface area and pore volume of ZnO/SBA-16 were found to be 188m^2/g and 0.50cm^3/g respectively. Average pore size and particle size were found to be 10.66nm and 31.84nm respectively. BET surface area is not as high as expected due to the incorporation of zinc oxide into SBA-16 mesoporous silica.

Table 1: Textual parameters of ZnO/SBA-16

Pore size (nm)	*Vp* (cm^3g^{-1})	Particle Size (nm)	S_{BET} (m^2g^{-1})
10.66nm	0.50cm^3/g	31.84nm	188m^2/g

3.5 Photo degradation activity

After characterization, the photo catalytic activity of as-prepared catalyst ZnO/SBA-16 was evaluated for the degradation of crystal violet and methylene blue dye. Degradation of both dyes was carried out under sunlight. In photo degradation experiments, there are two factors resulting in the decrease of the concentration of dyes: the adsorption of the dyes onto the surface of photo catalyst and the photo degradation of dyes.

Effects of different parameters such as time, dye concentration, change in pH, presence and absence of catalyst and light have been investigated. Degradation of both dyes was also carried out on parent SBA-16 without ZnO incorporation. In the absence of catalyst (ZnO/SBA-16), dyes showed high stability towards sunlight irradiation and no significant degradation was noticed as shown in Figure 8.

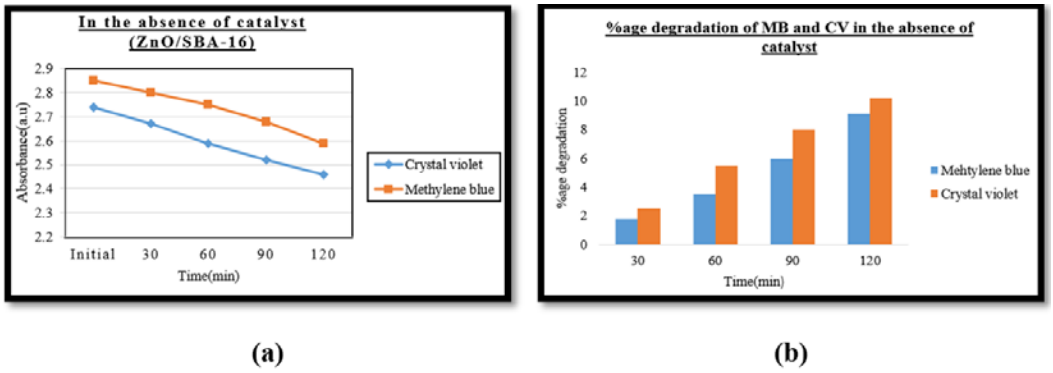

Fig 8: Degradation of dyes in the absence of catalyst

With parent SBA-16, only adsorption was observed as SBA-16 lacks active catalytic sites. 10% removal took place in case of methylene blue and 14% in case of crystal violet as shown in Figure 9.

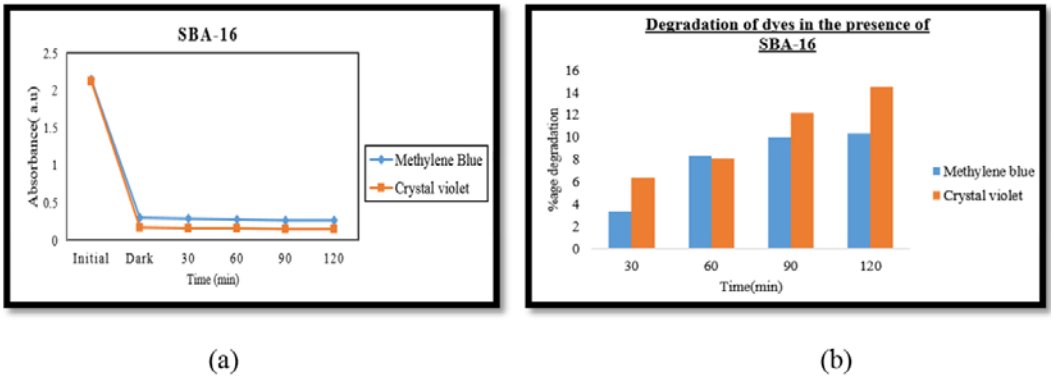

Fig 9: Removal of dyes in the presence of SBA-16

3.5.1 Effect of concentration

The photo catalytic degradation of both dyes at different initial concentration of dyes in the range from 15–50 ppm was studied. The conc. at which maximum degradation was observed with 30 mg of ZnO/SBA-16 is found to be 15 ppm for both dyes (97% in case of MB and 91% in case of CV) as shown in Figure 10.

Hence it can be concluded that catalyst exhibited greater degradation efficiency at low concentration of dye, because at high concentration more irradiation time and amount of catalyst was required to fully degrade the sample.

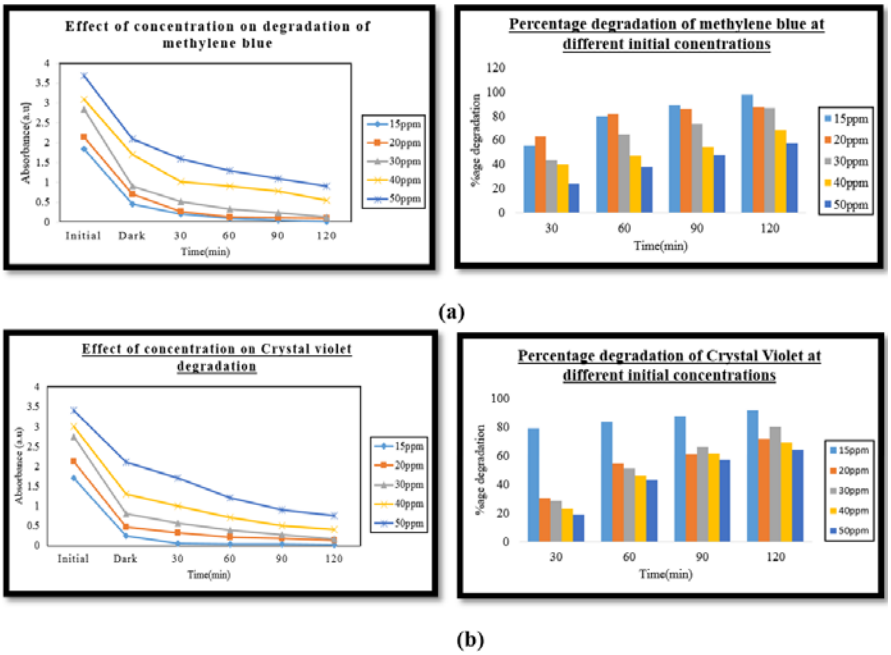

Fig 10 (a) and (b): Effect of conc. on degradation

3.5.2 Effect of time

The effect of irradiation time on degradation efficiency of both dyes was also investigated by keeping other parameters constant. During these photo degradation experiments, samples were irradiated under sunlight for 2 hours.

With increase in irradiation time, the degradation of both dyes was also found to increase. In case of crystal violet after first 30min of exposure only 28% percent degradation was observed while after 120min 80% degradation was observed. MB showed only 35% degradation after first 30min while after 120 min 86% removal was achieved as shown in Figure 12.

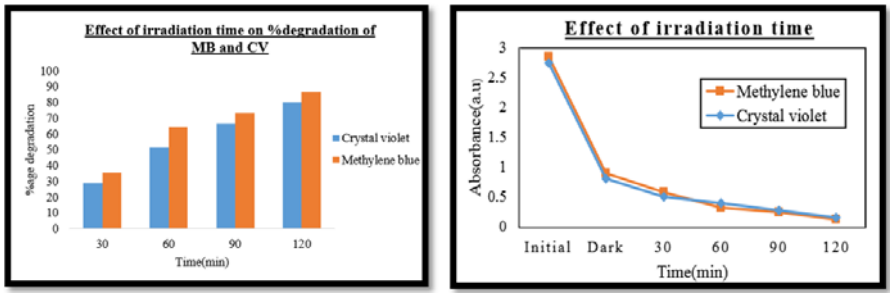

Fig 12: Effect of time on degradation of both dyes

3.5.3 Effect of pH

The pH has a great effect on degradation of dyes. The degradation experiments were carried out in the pH range 4–12. Both dyes are basic and showed little degradation in acidic medium.

As pH changed from acidic to basic medium percentage degradation of dye was increased and a marked decrease in the dye concentration was observed after 120min in all the samples. In the case of methylene blue maximum degradation was observed at pH 11 i.e. 100%. Methylene blue showed 87 percent removal within first 30 min of exposure to sunlight at pH 11 while at pH 4 only 69.9% removal was observed after 2hours as shown in Figure 13. In the case of crystal violet the maximum degradation was noted at pH 12 i.e. 100%. Crystal violet dye showed 88 percent degradation at pH 12 within first 30min while at pH 4 only 67% degradation was achieved after 120 min as shown in Figure 15.

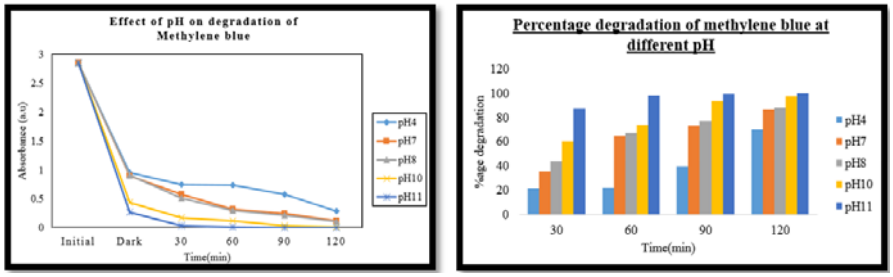

Fig 13: Effect of pH on degradation of methylene blue

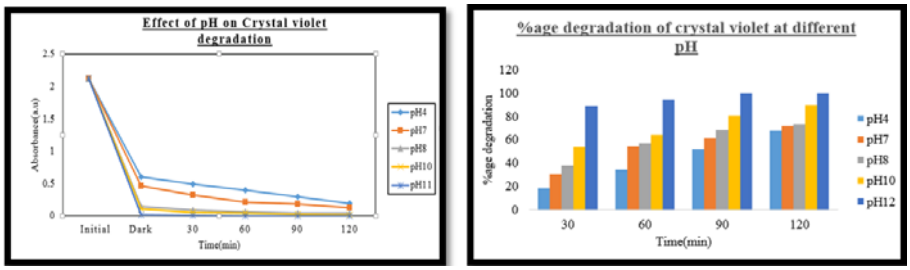

Fig 15: Effect of pH on degradation of crystal Violet

The dyes showed little degradation at low pH because surface of catalyst becomes positively charged in acidic medium which repels the cationic surface of dye making the adsorption and degradation difficult while at basic pH more hydroxide ions are available on the surface of catalyst that have high affinity for cationic dyes.

3.6 Kinetic study

In the present work kinetic study of removal of methylene blue and crystal violet by photocatalytic degradation was done using first order kinetic model at different initial concentrations of dyes and varying pH.

The best fitted model for the kinetic experimental data was selected using the linear regression correlation co-efficient, R^2 value.

In a photo degradation kinetic measurements, 50ml of the dye solution of various concentrations were taken and a known amount of photocatalyst was added in solution. Prior to photocatalytic experiments, solutions were stirred under dark in order to achieve adsorption-desorption equilibrium. Irradiation was carried out under sunlight for about 2h.

Few ml of sample solution was collected before and at regular intervals for analysis during irradiation. Catalyst was removed by centrifugation. The absorbance of the dye was measured using UV-Vis spectrophotometer.

3.6.1 First Order Kinetics

It has been reported that the rate of photo degradation of organic compounds follows the first order kinetics. Hence in the present work Pseudo first order kinetic model is used to find the rate of degradation of CV and MB dye. First order model is expressed as equation (1).

$$\ln C_t / C_o = -kt \quad (1)$$

Where C_t represents the concentration at time t, C_o represents the initial concentration and k is the rate constant. The first order rate constant $K_1$is determined from the slope.

A linear plot of ln (C_t/C_o) against time allows one to obtain the first order rate constant for degradation of dyes. Figure 17 (a) and (b) shows first order kinetics of MB and Figure 18 (a) and (b) shows first order kinetics of CV at different initial dye concentrations and varying pH respectively.

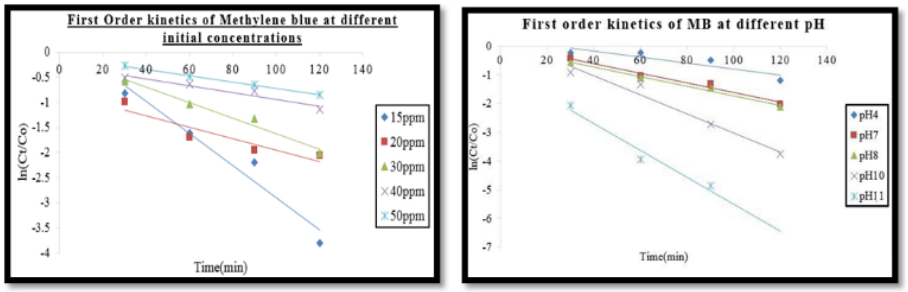

(a) **(b)**

Fig 17: First order kinetics of MB dye (a) Various initial dye conc. (b) Varying pH

The rate constants, half-life and the corresponding correlation coefficients for all concentrations and pH have been calculated and summarized in Table 2 and 3. The experimental data showed a good compliance with the First-order equation and the correlation coefficients for the linear plots were above 0.90 for almost all the experimental data. This suggested that the degradation of both dye obeys 1st-order mechanism.

It was observed that percentage degradation decreases with increase in dye concentration and the highest rate constant was observed at 15ppm for both dyes.

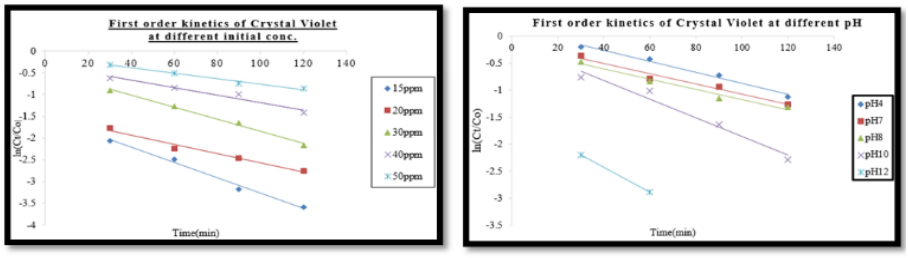

(a) **(b)**

Fig 18: First order kinetics of CV dye (a) Various initial dye conc. (b) Varying pH

3.6.2 Half-life determination

Half-life of MB and CV was calculated under different conditions. When the concentration was reduced to 50 % of the initial amount, half-life ($t_{1/2}$) was determined as

$t_{½} = 0.693/k$

Where k is the degradation constant.

From Table 2 (a) it can be seen that half-life reduced from 110min to 21.5min as initial dye concentration decreases.

Table 2: First order parameters for removal of MB (a) at different initial dye conc. (b) at different pH

(a)

Initial dye conc.	Pseudo 1st order		
	R^2	k_1/min	T ½ (min)
15	0.9502	0.0319	21.7
20	0.8682	0.0115	60.2
30	0.9728	0.0154	45.0
40	0.9259	0.0068	101
50	0.9984	0.0063	110

(b)

pH	Pseudo 1st order		
	R^2	k_1/min	T 1/2 (min)
4	0.806	0.010	69.3
7	0.978	0.016	43.3
8	0.988	0.016	43.3
10	0.964	0.033	21
11	0.961	0.046	15.0

Table 3: First order parameters for removal of CV (a) at different initial dye conc. (b) at different pH

(a)

Initial dye conc.	Pseudo 1st order		
	R^2	k_1/min	T ½ (min)
15	0.9812	0.0176	39.3
20	0.9978	0.0110	63
30	0.9717	0.0140	49.5
40	0.9899	0.0085	81.5
50	0.9781	0.0063	110

(b)

pH	Pseudo 1st order		
	R^2	k_1/min	T 1/2 (min)
4	0.9826	0.0103	67.2
7	0.971	0.0095	72.9
8	0.976	0.0094	73.7
10	0.967	0.0172	40.2
12	1	0.0231	32.5

6. Catalyst Regeneration

ZnO/SBA-16 catalyst was recovered from methylene blue solution by filtration using sintered glass crucible and subsequent calcination at 550 °C for 2h was carried out. The recovered catalyst was characterized by FTIR and its catalytic efficiency for the removal of methylene blue was investigated. The results showed that 86% degradation of methylene blue was achieved after 120min at pH 11.

Hence the catalyst exhibit good photo degradation ability even after regeneration. However, fresh catalyst was slightly more efficient than the regenerated one.

7. Supplementary Information

7.1 FT-IR spectrum of recovered catalyst

Figure 19 shows FTIR spectrum of recovered catalyst. The band at 462cm^{-1} and 809cm^{-1} corresponds to the symmetric bending and stretching vibrations for Si-O-Si bonds.

The peak at 1087cm^{-1} was assigned to the asymmetric stretching vibration of Si-O-Si bond.

Hence it can be seen that mesoporous silica SBA-16 retained its Si-O-Si framework even after regeneration and it is similar to that of fresh one. No peaks shifting is observed in case of recovered catalyst.

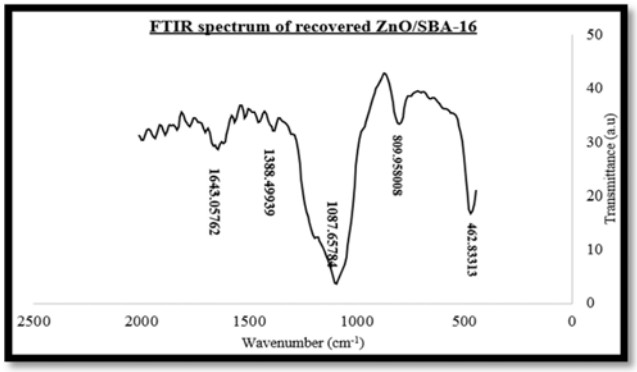

Fig 19: FT-IR spectrum of recovered ZnO/SBA-16 catalyst

7.2 Evaluation of catalytic efficiency of recovered catalyst

The catalytic efficiency of regenerated catalyst was tested for methylene blue at pH 11 as shown in Figure 21. The results showed that 86% degradation of methylene blue was achieved after 120min at pH 11.

Hence the catalyst exhibit good photo degradation ability even after regeneration. However, fresh catalyst was slightly more efficient than the regenerated one.

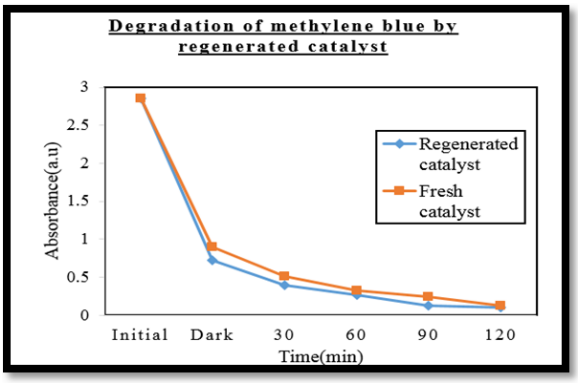

(a)

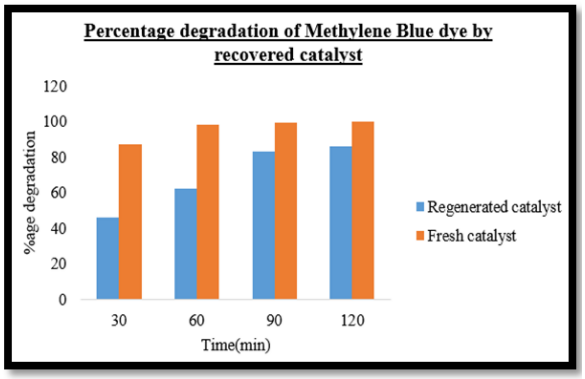

(b)

Fig 21: (a) and (b) shows degradation of methylene blue by regenerated catalyst

8. Conclusion

SBA-16 mesoporous silica was successfully prepared under reflux using Pluronic F127 surfactant as template and CTAB as co-template. It was suggested that CTAB reduces reaction time and helps in regulating size and morphology of pores of SBA-16 by increasing micellization of Pluronic F127 surfactant.

The catalytic activity of as prepared ZnO/SBA-16 catalyst was evaluated for degradation of methylene blue. The results revealed that ZnO/SBA-16 showed excellent photo degradation efficiency towards MB dye.

Photo degradation results were dependent on the irradiation time, concentration of dye and pH. At lower concentration of dyes better degradation was observed. By increasing irradiation time degradation was also increased. Both dyes showed better degradation in basic pH. From the above mentioned results we can conclude that as synthesized zinc oxide incorporated SBA-16 is an excellent catalyst.

9. References

1. Acosta SYJ, Nava R, Hernandez MV, Macias SSA, Gomez HML, Pawelec B. Methylene blue photo degradation over titania-decorated SBA-15 Appl. Catal. B: Environ. 2011; 110:108-117
2. Miclescu, A., Wiklund, L., Roman, J., Anestezie, d., Intensiva, T. 2010; 17: 35
3. Mohammed MA, Shitu A, Ibrahim A. Res J Chem Sci. 2014; 4:91.
4. Voa V, Thib TPT, Kima H, Kima SJ, Vo V. Facile post-synthesis and photocatalytic activity of N-doped ZnO–SBA-15 J Phys Chem Solids. 2014; 75(3):403-409.
5. Dai P, Zhanga L, Zhanga G, Lia G, Suna Z, Liu X *et al*. Characterization and photocatalytic activity of (ZnO–CuO)/SBA-15 nanocomposites synthesized by two-solvent method Mater. Res. Bull. 2014; 56:119-124.
6. Mihai GD, Meynen V, Mertens M, Bilba N, Cool P, Vansan EF. Zn O nanoparticles supported on mesoporous MCM-41 and SBA-15: a comparative physicochemical and photocatalytic study J Mater Sci. 2010; 45(21):5786-5794
7. Ryoo R, Ko CH, Kruk M, Antochshuk V, Jaroniec M. Block-Copolymer-Templated Ordered Mesoporous Silica: Array of Uniform Mesopores or Mesopore−Micropore Network J Phys Chem B. 2000; 104:11465-11471.
8. Sun H, Tang Q, Du Y, Liu X, Chen Y, Yang Y. Mesostructured SBA-16 with excellent hydrothermal, thermal and mechanical stabilities: Modified synthesis and its catalytic application J Colloid Interf Sci. 2009; 333:317-323.
9. Wang X, Sun T, Yang J, Zhao L, Jia J. Low-temperature H_2S removal from gas streams with SBA-15 supported ZnO nanoparticles Chem. Eng J. 2008; 142:48-55.
10. Andrade GF, Soares DCF, Santos RGD, Sousa EMB, Andrade GF. Mesostructured SBA-16 with excellent hydrothermal, thermal and mechanical stabilities: Modified synthesis and its catalytic application Micropor. Mesopor. Mater. 2013; 168:102-110.